Constraining Gluonic Quartic Gauge Coupling Operators with $gg \to \gamma\gamma$

John Ellis
Theoretical Particle Physics and Cosmology Group, Physics Department, King's College London, London WC2R 2LS, United Kingdom,
National Institute of Chemical Physics and Biophysics, Rävala 10, 10143 Tallinn, Estonia,
and Theoretical Physics Department, CERN, CH-1211 Geneva 23, Switzerland

Shao-Feng Ge
Kavli IPMU, UTIAS, University of Tokyo, Kashiwa, Chiba 277-8583, Japan,
and Department of Physics, University of California, Berkeley, California 94720, USA

(Received 12 February 2018; revised manuscript received 15 May 2018; published 23 July 2018)

Gluon-gluon to photon-photon scattering $gg \to \gamma\gamma$ offers to the LHC experiments a uniquely powerful probe of dimension-8 operators in the standard model effective field theory that are quadratic in both the electromagnetic and gluonic field-strength tensors, such as would appear in the Born-Infeld extension of the standard model. We use 13-TeV ATLAS data on the production of isolated photon pairs to set lower limits on the scales of dimension-8 operators $M \gtrsim 1$ TeV and discuss the prospective sensitivities of possible future hadron colliders.

DOI: 10.1103/PhysRevLett.121.041801

Introduction.—A model-independent way to constrain possible extensions of the standard model (SM) with high-scale new physics that decouples at low energies is provided by the standard model effective field theory (SMEFT) [1], which employs a systematic expansion in the effective mass dimensions of the new operators generated by high-scale physics beyond the SM. Apart from the dimension-5 operators that may contribute to neutrino masses and oscillations [2], the most prominent operators are those of dimension 6, whose coefficients scale as $1/\Lambda^2$, where Λ represents a generic new-physics scale. There have been many studies of the constraints on dimension-6 operator coefficients imposed by current and potential future collider data [3]. Some attention has also been paid to the experimental constraints on operators of dimension $d \gtrsim 8$, whose effects at low energies are suppressed by $\mathcal{O}(E/\Lambda)^{d-4}$, particularly those involving four electroweak gauge field strengths; see, e.g., Refs. [4,5].

We focus here on dimension-8 operators in the SMEFT that are quadratic in the field-strength tensors of both the gluon fields of QCD, $G^a_{\mu\nu}: a = 1, \ldots, 8$, and electroweak gauge fields, either the $W^i_{\mu\nu}: i = 1, 2, 3$ of SU(2) or the $B_{\mu\nu}$ of U(1). As we review in more detail below, there are 8 independent such dimension-8 operators, 4 involving pairs of the $W^i_{\mu\nu}$ and 4 involving pairs of $B_{\mu\nu}$. Since the electromagnetic field strength tensor $F_{\mu\nu}$ is a specific combination of $W^3_{\mu\nu}$ and $B_{\mu\nu}$, the $gg \to \gamma\gamma$ scattering process is sensitive to just 4 combinations of these dimension-8 operators.

One of these combinations is of particular interest, as it arises in the Born-Infeld (BI) extension of the SM with the following Lagrangian $\mathcal{L}_{\mathrm{BISM}}$:

$$\beta^2\left[1-\sqrt{1+\sum_{\lambda=1}^{12}\frac{F^{\lambda}_{\mu\nu}F^{\lambda,\mu\nu}}{2\beta^2}-\left(\sum_{\lambda=1}^{12}\frac{F^{\lambda}_{\mu\nu}\tilde{F}^{\lambda,\mu\nu}}{4\beta^2}\right)^2}\right], \quad (1)$$

where $\beta \equiv M^2$ is the BI nonlinearity scale and the index λ runs over the 12 generators of the SM $\mathrm{SU}(3) \times \mathrm{SU}(2) \times \mathrm{U}(1)$ gauge group. Born and Infeld proposed a similar nonlinear extension of QED in 1934 [6], motivated by a "unitarian" idea that there should be an upper limit on the strength of the electromagnetic field. However, this theory remained largely a curiosity until Fradkin and Tseytlin [7] showed in 1985 that it appears in models inspired by M theory, e.g., in which vector fields are coupled to matter particles that are localized on lower-dimensional "branes" [8]. We note also that it has recently been shown that BI theories have uniquely soft scattering amplitudes in the infrared limit [9].

It was pointed out in Ref. [10] that a measurement of light-by-light scattering in heavy-ion collisions at the LHC by the ATLAS Collaboration [11] imposes a constraint on the BI extension of QED that is orders of magnitude

stronger than that available from previous, lower-energy experiments [12], corresponding, e.g., in the context of M theory to an upper limit on the separation between branes $\lesssim 1/(100\ \mathrm{GeV})$. The purpose of this Letter is to show that an ATLAS measurement of $gg \to \gamma\gamma$ scattering in proton-proton collisions [13] strengthens this limit by almost another order of magnitude in the context of a BI extension of the SM. This bound penetrates significantly the parameter space of variants of M theory with large extra dimensions [8], and we show how future hadron colliders would offer even greater sensitivity.

Dimension-8 gluon or photon operators.—Constructing the effective operators that contribute to $gg \to \gamma\gamma$ scattering needs two gluon fields and two photon fields [14]. Since fermions and massive vector bosons are absent in the external states of this process, the candidate operators involve only these fields, appearing via the gluon field strength $G^a_{\mu\nu}$ and the photon field strength $F_{\mu\nu}$, which is a combination of the $B_{\mu\nu}$ of $\mathrm{U}(1)_Y$ and the $W^3_{\mu\nu}$ of $\mathrm{SU}(2)_L$ with coefficients $s_W \equiv \sin\theta_W$ and $c_W \equiv \cos\theta_W$, respectively. The dimension-8 operators relevant to $gg \to \gamma\gamma$ scattering require two gluon field strengths $G^a_{\mu\nu}$ and two electroweak field strengths $B_{\mu\nu}$ or $W^i_{\mu\nu}$. The two color indices a must be contracted, as must the two $\mathrm{SU}(2)_L$ indices i. Lorentz invariance allows 4 different ways of contracting the 8 space-time indices. Thus there are 8 independent gluonic quartic gauge coupling (gQGC) operators, and the relevant dimension-8 part of the effective Lagrangian may be written as $\mathcal{L}_{gT} = \sum_{i=0}^{7}(1/16\beta_i^2)\mathcal{O}_{gT,i}$, where

$$\mathcal{O}_{gT,0} = \sum_a G^a_{\mu\nu}G^{a,\mu\nu} \times \sum_i W^i_{\alpha\beta}W^{i,\alpha\beta}, \tag{2a}$$

$$\mathcal{O}_{gT,1} = \sum_a G^a_{\alpha\nu}G^{a,\mu\beta} \times \sum_i W^i_{\mu\beta}W^{i,\alpha\nu}, \tag{2b}$$

$$\mathcal{O}_{gT,2} = \sum_a G^a_{\alpha\mu}G^{a,\mu\beta} \times \sum_i W^i_{\nu\beta}W^{i,\alpha\nu}, \tag{2c}$$

$$\mathcal{O}_{gT,3} = \sum_a G^a_{\alpha\mu}G^a_{\beta\nu} \times \sum_i W^{i,\mu\beta}W^{i,\nu\alpha}, \tag{2d}$$

$$\mathcal{O}_{gT,4} = \sum_a G^a_{\mu\nu}G^{a,\mu\nu} \times B_{\alpha\beta}B^{\alpha\beta}, \tag{2e}$$

$$\mathcal{O}_{gT,5} = \sum_a G^a_{\alpha\nu}G^{a,\mu\beta} \times B_{\mu\beta}B^{\alpha\nu}, \tag{2f}$$

$$\mathcal{O}_{gT,6} = \sum_a G^a_{\alpha\mu}G^{a,\mu\beta} \times B_{\nu\beta}B^{\alpha\nu}, \tag{2g}$$

$$\mathcal{O}_{gT,7} = \sum_a G^a_{\alpha\mu}G^a_{\beta\nu} \times B^{\mu\beta}B^{\nu\alpha}, \tag{2h}$$

where the scales $\sqrt{\beta_i} \equiv M_i$ represent the scales of the physics beyond the SM that induces these effective operators. Operators of the form similar to $\mathcal{O}_{gT,3}$ and $\mathcal{O}_{gT,7}$ have not been discussed in the context of electroweak QGCs [4]. The effective Lagrangian for $gg \to \gamma\gamma$ scattering may be written in the form $\hat{\mathcal{L}}_{gT} = \sum_{i=0}^{3}(1/16\hat{\beta}_i^2)\hat{\mathcal{O}}_{gT,i}$, where $(1/\hat{\beta}_i^2) \equiv (s_W^2/\beta_i^2) + (c_W^2/\beta_{i+4}^2)$, $i = 0,\ 1,\ 2,\ 3$ and the $\hat{\mathcal{O}}_{gT,i}$ have the same forms as the $\mathcal{O}_{gT,i}$, $i = 4, 5, 6, 7$ but with $B_{\alpha\beta}$ replaced by $F_{\alpha\beta}$.

The first term in the BI extension Eq. (1) of the SM generates $\mathcal{O}_{gT,0}$ and $\mathcal{O}_{gT,4}$, and hence also $\hat{\mathcal{O}}_{gT,0}$. The second term in Eq. (1) yields a quartic interaction with the Lorentz structure $(W_{\mu\nu}\tilde{W}^{\mu\nu})(G_{\alpha\beta}\tilde{G}^{\alpha\beta}) = -2(W_{\mu\nu}G^{\mu\nu})^2 + 4(W_{\mu\nu}G^{\nu\alpha}W_{\alpha\beta}G^{\beta\mu})$, where the SU(2) and color indices have been omitted, and similarly with $W \to B$, generating $\mathcal{O}_{gT,1}$, $\mathcal{O}_{gT,5}$ and $\mathcal{O}_{gT,3}$, $\mathcal{O}_{gT,7}$, and hence also $\hat{\mathcal{O}}_{gT,1}$, $\hat{\mathcal{O}}_{gT,3}$. One would expect the coefficients $(1/\beta_0^2)$ and $(1/\beta_4^2)$ to be equal at the common BI scale $M_0 = M_4$, but subject to different renormalization below that scale, and similarly for $i = 1$, 3 and 5,7. However, since the constraint we find on the BI scale is not very different from the electroweak scale, this effect is small and we neglect it in our analysis. In this approximation, the experimental constraints on M_0 that we derive below are proxies for the corresponding constraints on the BI scale $M = \sqrt{\beta}$.

$gg \to \gamma\gamma$ scattering.—The different Lorentz structures in Eq. (2) yield different cross sections for the $gg \to \gamma\gamma$ process [15]:

$$\frac{d\sigma_{gT,i}}{dt} = \frac{(s_W^4, c_W^4)}{\beta_i^4} \begin{cases} \frac{s^2}{4096\pi} & i = 0, 4 \\ \frac{s^4 - 2s^2(t^2+u^2) + 3(t^4+u^4)}{32768\pi s^2} & i = 1, 5 \\ \frac{2s^4+t^4+u^4}{131072\pi s^2} & i = 2, 6 \\ \frac{s^4+t^4+u^4+4t^2u^2}{131072\pi s^2} & i = 3, 7, \end{cases}$$

where $s \equiv (p_{\gamma_1} + p_{\gamma_1})^2$, $t \equiv (s/2)(\cos\theta - 1)$, and $u \equiv -t - s$ are Mandelstam variables. The four different Lorentz structures have different dependences on the scattering angle θ in the center-of-mass frame, independent of s, as shown in the upper panel of Fig. 1. Once an excess beyond the SM background is seen, the Lorentz structures can be identified by fitting the θ distribution. These angular dependences can be contrasted with that of the SM $q\bar{q} \to \gamma\gamma$ background: $d\sigma/d\cos\theta \propto \cot^2\theta$ that vanishes for $\theta = \pi/2$ in the massless limit. A cut on the angular distribution $|\cos\theta| \leq 0.8$ or 0.9 (equivalent to a cut in pseudorapidity) would be effective for suppressing the SM background.

Each gauge field contributes a momentum factor to the amplitudes generated by the dimension-8 gQGC operators Eq. (2), so the total cross sections scale as s^3

$$\sigma_{gT,i} = \frac{(s_W^4, c_W^4)}{4096\pi\beta_i^4} \times \left(1, \frac{13}{120}, \frac{3}{40}, \frac{23}{480}\right) \times s^3. \tag{3}$$

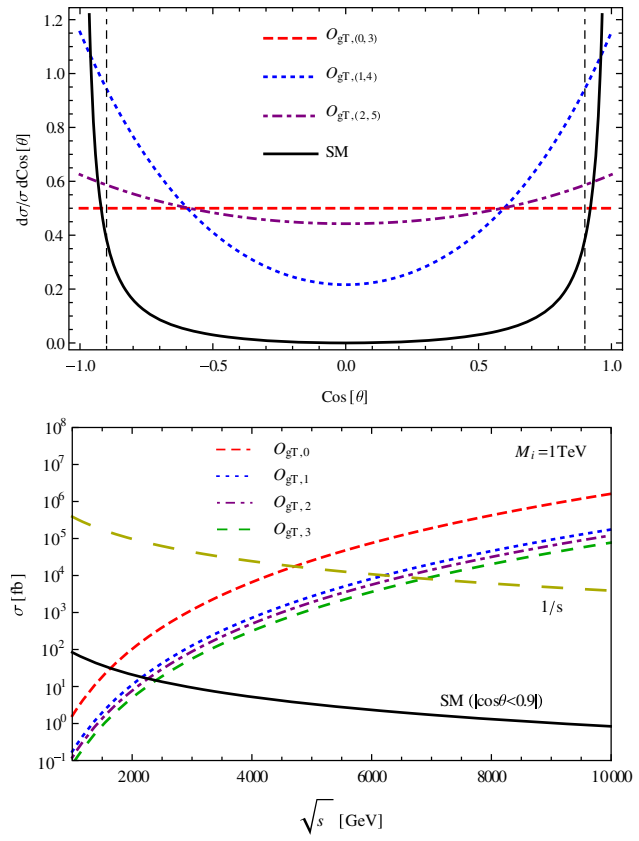

FIG. 1. Angular distributions in the center-of-mass frame of $gg \to \gamma\gamma$ scattering (upper panel) and the corresponding total cross sections (lower panel), where a cut $|\cos\theta| < 0.9$ on the scattering angle in the center-of-mass frame has been used to regularize the SM cross section.

The cross sections for $\mathcal{O}_{gT,(1,5)}$, $\mathcal{O}_{gT,(2,6)}$, and $\mathcal{O}_{gT,(3,7)}$ are roughly 1 order smaller than those for $\mathcal{O}_{gT,(0,4)}$, respectively. Considering the s_W^4 and c_W^4 coefficients, the contributions of the eight gQGC operators have a hierarchical structure: $\sigma_{gT,4} \approx 10\sigma_{gT,(0,5,6,7)} \approx 100\sigma_{gT,(1,2,3)}$ for identical scales of M_i.

A characteristic energy of $gg \to \gamma\gamma$ scattering at LHC-13 TeV is $\mathcal{O}(1)$ TeV, which places a natural limit on the applicability of gQGC operators. If $\sqrt{s}$ exceeds M_i, the $\mathcal{O}_{gT,i}$ operators would eventually cease to be a good approximation, violating the unitarity constraint. To preserve unitarity, we assume that the cross section falls with the diphoton invariant mass, $\sigma \approx 1/s = 1/m_{\gamma\gamma}^2$, above the scales $\sqrt{s_i}$ where unitarity is saturated:

$$\sqrt{s_i} = M_i \left[\frac{(s_W^4, c_W^4)}{4096\pi} \left(1, \frac{13}{120}, \frac{3}{40}, \frac{23}{480}\right) \right]^{-1/8}, \quad (4)$$

corresponding to ratios $\sqrt{s_i}/M_i = 4.71$, 6.21, 6.51, 6.88, 3.49, 4.60, 4.82, 5.10 for $i = 0, \ldots, 7$. The cross section increases as s^3 below and decreases as $1/s$ above the saturation point.

The cross section for the SM background $q\bar{q} \to \gamma\gamma$ also falls with energy: at leading order, $\sigma_{\mathrm{SM}} \approx \sum_q Q_q^4 \{\log[1/(1-\cos\theta_{\mathrm{cut}})] - 2\}/24\pi s$, where Q_q is the electric charge and θ_{cut} is a cut $|\cos\theta| < \cos\theta_{\mathrm{cut}} = 0.9$ on the scattering angle in the center-of-mass frame. Higher-order QCD corrections increase this by a slowly varying K factor [16], yielding results in agreement with the ATLAS measurements [13]. The lower panel of Fig. 1 compares this background with the gQGC signals for $M_i = 1$ TeV. The SM background lies far below the scale of unitarity saturation, and falls below the potential gQGC signals when $\sqrt{s} \sim 2$–3 TeV. In addition to exploiting the different angular distribution, one may also suppress the SM background by cutting low $\sqrt{s}$ events.

Constraints from the ATLAS data.—The ATLAS Collaboration searched for new physics with high-mass diphoton final states [13]. Comparing their searches for spin-0 and -2 resonant and nonresonant signals, the nonresonant case is the closest in spirit to the gQGC contribution to $gg \to \gamma\gamma$ that we consider here.

The ATLAS analysis uses the fiducial region $|\eta| < 2.37$, excluding the blind transition region $1.37 < |\eta| < 1.52$. In the nonresonant signal search, the photon transverse energies receive a cut $E_T > 55$ GeV. For nonresonant Kaluza-Klein signal, the geometric acceptance increases from 58% at $M_S = 3.5$ TeV to 65% at $M_S = 5$ TeV, where M_S is the cutoff scale of the Kaluza-Klein spectrum.

In our analysis, we assume a constant geometric acceptance of 60%, which is to be combined with the efficiency for reconstruction and identification that is approximately constant at 77%, yielding an overall signal event selection efficiency of 46%. The upper panel of Fig. 2 shows the expected signal event rates at ATLAS with 36.7 fb^{-1} and 13 TeV for the different gQGC operators with $M_i =$ 1 TeV, as functions of the invariant mass $m_{\gamma\gamma}$ [17,18]. For comparison, we also show the background rate extracted from the background-only fit in Fig. 2(b) of Ref. [13]. With cutoff scale $M_i = 1$ TeV, the background and gQGC signals cross around $m_{\gamma\gamma} = 1$–2 TeV, as expected from Fig. 1. Above $m_{\gamma\gamma} = 1.5$ TeV, the signal rate keeps rising before saturating unitarity at $m_{\gamma\gamma} \gtrsim 4$ TeV, depending on the model. In our estimations of the SM background and signals we use the cut $m_{\gamma\gamma} < 2$ TeV, well below these unitarity saturation scales.

With this cut, we make a binned analysis of the ATLAS data [13] to quantify the sensitivity $\sum_i |S_i + B_i - N_i|/\sqrt{N_i}$ to these operators, where S_i and B_i are the predicted total signal and background while N_i is the number of events actually measured in the ith bin. We plot the significances, evaluated using the $\Delta\chi^2$ distributions, as functions of the nonlinearity scale M_i in the lower panel of Fig. 2. The significances decrease very rapidly with M_i. Since the gQGC operator coefficients are suppressed by $1/M_i^4$, the cross sections fall as $1/M_i^8$ and small changes in

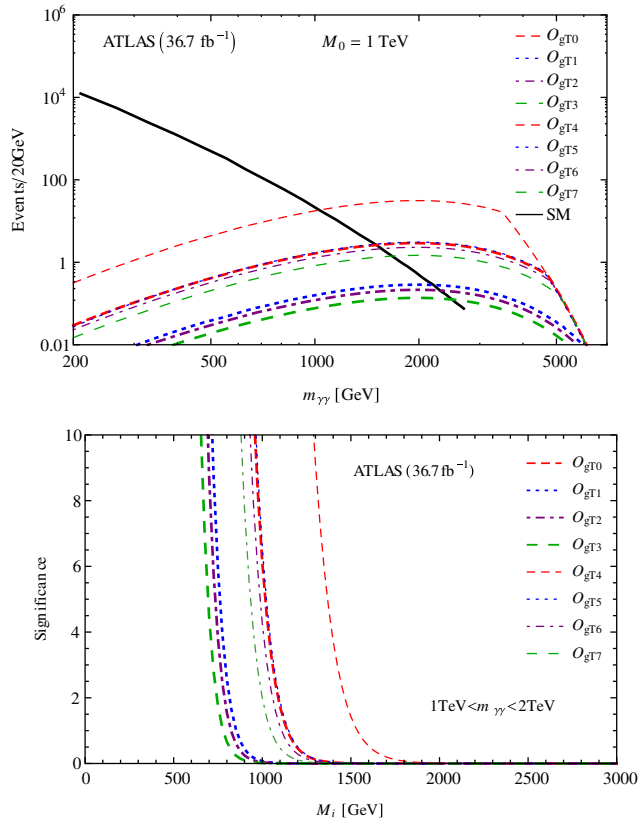

FIG. 2. Event spectra (upper panel) and sensitivities (lower panel) of ATLAS with 36.7 fb^{-1}.

the M_i can affect the significances dramatically. The hierarchical structure of the cross sections generated by the eight gQGC operators is manifest in the 95% C.L. lower bounds derived from the ATLAS data: $M_i \gtrsim (1040, 777, 750, 709, 1399, 1046, 1010, 954)$ GeV [19]. We recall that M_0 is a proxy for the SM BI scale M. Note that setting a 2 TeV upper cut on invariant mass $m_{\gamma\gamma}$ is roughly the same as shifting the saturation point down to $\sqrt{s_i} = 2$ TeV.

Sensitivities at future hadron colliders.—As discussed analytically above, the most effective cut for suppressing the SM background is that on the scattering angle in the center-of-mass frame. Figure 3 shows the cross sections obtained with different cuts on the angular distributions, applying the fiducial cut $|\eta(\gamma)| < 2.37$ in all cases. In comparison, the black curves were obtained with the ATLAS E_T cut, $E_T(\gamma) > 55$ GeV. Across the whole invariant-mass region, the scattering angle cut can reduce significantly the SM background, with much smaller effects on the signals. Therefore, the scattering angle cut in the center-of-mass frame is more suitable than E_T cut for the search for dimension-8 gQGC operators. In the following discussion of the sensitivities at future colliders, we apply cuts $|\eta(\gamma)| < 2.37$ and $|\cos\theta(\gamma)| < 0.8$.

The upper panel of Fig. 4 shows how the SM background (thinner lines) and the gQGC signals (thicker lines) change

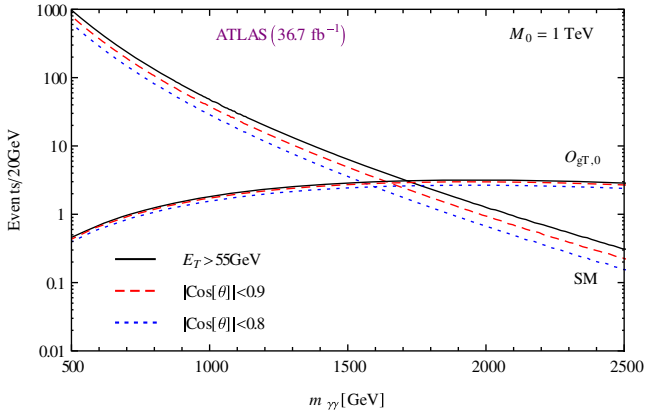

FIG. 3. The effects of E_T and $\cos\theta$ cuts for the ATLAS search.

with collider energy. For illustration, we only plot $\mathcal{O}_{gT,0}$ whose features are shared by other gQGC operators. For comparison, we use the same luminosity 36.7 fb^{-1} for different collider energies, noting that the event rates would be much larger for the expected luminosities at HE-LHC at 27 TeV [20], FCC-hh [21], and SppC [22]. At higher energies the signal event spectra are significantly enhanced, especially in the high $m_{\gamma\gamma}$ range. For $\sqrt{s} = 100$ TeV, the event rate can be as large as $10^4/20$ GeV for $M_i = 1$ TeV. Although the SM background also increases, its contribution at high $m_{\gamma\gamma}$ range is still negligibly small. At higher collider energies $\sqrt{s}$, the crossing point between the SM background and the gQGC signal curves decreases. The crossings for $\sqrt{s} = (13, 27, 50, 100)$ TeV happen at $m_{\gamma\gamma} = (1.60, 1.32, 1.17, 1.06)$ TeV. We increase the upper cut on the invariant mass roughly proportionally to the collider energy: $m_{\gamma\gamma} \leq (3, 5, 9, 14)$ TeV, respectively.

The lower panel of Fig. 4 shows the significances $\sum_i S_i/\sqrt{S_i + B_i}$ at various hadron colliders, including LHC at 13 TeV with 3 ab^{-1}, HE-LHC at 27 TeV, and FCC-hh and SppC at 50 or 100 TeV, each with 20 ab^{-1} for the $\mathcal{O}_{gT,0}$ operator. Enhancing collider energy and luminosity significantly improves the sensitivity. The 3σ discovery sensitivity can reach 2.1 TeV at 3 ab^{-1} LHC, 4.5 TeV at the 27-TeV HE-LHC, 7.5 TeV at the 50-TeV versions, and 13 TeV at the 100-TeV versions of FCC-hh and SppC. For FCC-hh and SppC at 100 TeV, the sensitivity would be another order of magnitude better than the current ATLAS analysis with 36.7 fb^{-1} at 13 TeV, well into the range of potential interest to string models.

Conclusions.—The ATLAS data on light-by-light scattering in heavy-ion collisions can exclude the QED BI [6] scale $\lesssim$100 GeV [10]. In this Letter, we have shown that the ATLAS data on $gg \to \gamma\gamma$ scattering enhance the sensitivity by an order of magnitude, to $\gtrsim$1 TeV for the analogous dimension-8 operator scales containing other combinations of gluon and electromagnetic fields. This constraint on the BI extension of SM is very interesting in

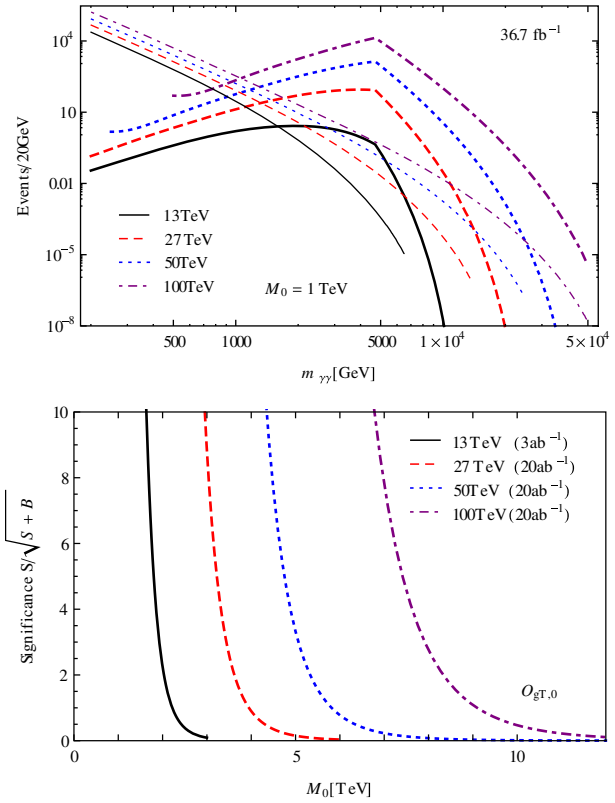

FIG. 4. The event spectra (upper panel) and sensitivities (lower panel) at future hadron colliders.

view of its connections with string theory [7] and particularly models in which branes are separated by distances $\gtrsim 1$ TeV^{-1} [8]. Moreover, similar searches for $\gamma\gamma$ production at possible future proton-proton colliders could be sensitive to BI scales in the multi-TeV scale, complementing the searches via dimension-6 SMEFT operators [23].

We thank Sasha Belyaev for useful discussions and Alexander Pukhov for help with CalcHEP. The work of J. E. was supported partly by the STFC Grant No. ST/L000258/1, and partly by the Estonian Research Council via a Mobilitas Pluss grant. The work of S.-F. G. was supported by World Premier International (WPI) Research Center Initiative, MEXT, Japan, and JSPS KAKENHI Grant No. JP18K13536.

[1] W. Buchmuller and D. Wyler, Nucl. Phys. **B268** (1986) 621.
[2] S. Weinberg, Phys. Rev. Lett. **43**, 1566 (1979).
[3] See D. de Florian *et al.* (LHC Higgs Cross Section Working Group), Handbook of LHC Higgs cross sections: 4. Deciphering the nature of the Higgs sector, CERN Yellow Reports, DOI: 10.23731/CYRM-2017-002 (2017), and references therein.
[4] O. J. P. Eboli, M. C. Gonzalez-Garcia, and J. K. Mizukoshi, Phys. Rev. D **74**, 073005 (2006), and references therein.
[5] D. R. Green, P. Meade, and M. A. Pleier, Rev. Mod. Phys. **89**, 035008 (2017); M. Rauch, arXiv:1610.08420.
[6] M. Born and L. Infeld, Proc. R. Soc. A **144**, 425 (1934).
[7] E. S. Fradkin and A. A. Tseytlin, Phys. Lett. **163B**, 123 (1985).
[8] For a review and references see A. A. Tseytlin, in *The Many Faces of the Superworld*, edited by M. A. Shifman (World Scientific, Singapore, 2000), pp. 417–452, DOI: 10.1142/4332.
[9] C. Cheung, K. Kampf, J. Novotny, C. H. Shen, J. Trnka, and C. Wen, Phys. Rev. Lett. **120**, 261602 (2018).
[10] J. Ellis, N. E. Mavromatos, and T. You, Phys. Rev. Lett. **118**, 261802 (2017).
[11] M. Aaboud *et al.* (ATLAS Collaboration), Nat. Phys. **13**, 852 (2017).
[12] J. Rafelski, G. Soff, and W. Greiner, Phys. Rev. A **7**, 903 (1973); H. Carley and Michael K.-H. Kiessling, Phys. Rev. Lett. **96**, 030402 (2006); S. Z. Akhmadaliev*et al.*, Phys. Rev. Lett. **89**, 061802 (2002); J. M. Dávila, C. Schubert, and M. A. Trejo, Int. J. Mod. Phys. A **29**, 1450174 (2014); S. Mereghetti, Astron. Astrophys. Rev. **15**, 225 (2008); F. D. Valle, E. Milotti, A. Ejlli, G. Messineo, L. Piemontese, G. Zavattini, U. Gastaldi, R. Pengo, and G. Ruoso, Phys. Rev. D **90**, 092003 (2014); M. Fouché, R. Battesti, and C. Rizzo, Phys. Rev. D **93**, 093020 (2016); **95**, 099902(E) (2017).
[13] M. Aaboud *et al.* (ATLAS Collaboration), Phys. Lett. B **775**, 105 (2017).
[14] Although the dimension-6 magnetic dipole operators $\bar{Q}\gamma^\mu W_{\mu\nu}D^\nu Q + \text{h.c.}$ and $\bar{Q}\gamma^\mu B_{\mu\nu}D^\nu Q + \text{h.c.}$ modify the $q\bar{q}A$ vertex, their prospective t-channel contribution to $q\bar{q} \to \gamma\gamma$ vanishes when the photons are on shell.
[15] PACKAGE-X: H. H. Patel, Comput. Phys. Commun. **197**, 276 (2015).
[16] S. Catani, L. Cieri, D. de Florian, G. Ferrera, and M. Grazzini, Phys. Rev. Lett. **108**, 072001 (2012); **117**, 089901(E) (2016); J. M. Campbell, R. K. Ellis, Y. Li, and C. Williams, J. High Energy Phys. 07 (2016) 148; S. Catani, L. Cieri, D. de Florian, G. Ferrera, and M. Grazzini, J. High Energy Phys. 04 (2018) 142.
[17] FEYNRULES: N. D. Christensen and C. Duhr, Comput. Phys. Commun. **180**, 1614 (2009); A. Alloul, N. D. Christensen, C. Degrande, C. Duhr, and B. Fuks, Comput. Phys. Commun. **185**, 2250 (2014).
[18] CALCHEP: A. Belyaev, N. D. Christensen, and A. Pukhov, Comput. Phys. Commun. **184**, 1729 (2013).
[19] We note that the range of validity of the effective field theory approach depends on various factors: see, e.g., J. Brehmer, A. Freitas, D. Lopez-Val, and T. Plehn, Phys. Rev. D **93**, 075014 (2016). For example, if a dimension-8 operator were generated by the exchange of some strongly coupled boson X with coupling $4\pi/M_X$, the SMEFT would be a good approximation up to an energy scale $E \sim M_X \sim \sqrt{4\pi}M_i \gtrsim 2$ TeV, covering the range of $m_{\gamma\gamma}$ used in our analysis for all the dimension-8 operators.
[20] See, for example, HE-LHC baseline parameters https://indico.cern.ch/event/556692/contributions/2590826/attachments/1469360/2272924/HE-LHC-Baseline-Parameters.pdf.
[21] See the Future Circular Collider Study https://fcc.web.cern.ch/Pages/default.aspx.
[22] See the CEPC-SppC Preliminary Conceptual Design Report http://cepc.ihep.ac.cn/preCDR/.

[23] J. Ellis and T. You, J. High Energy Phys. 03 (2016) 089; S. F. Ge, H. J. He, and R. Q. Xiao, J. High Energy Phys. 10 (2016) 007; S. F. Ge, H. J. He, and R. Q. Xiao, Int. J. Mod. Phys. A **31**, 1644004 (2016); J. Ellis, P. Roloff, V. Sanz, and T. You, J. High Energy Phys. 05 (2017) 096; G. Durieux, C. Grojean, J. Gu, and K. Wang, J. High Energy Phys. 09 (2017) 014; T. Barklow, K. Fujii, S. Jung, R. Karl, J. List, T. Ogawa, M. E. Peskin, and J. Tian, Phys. Rev. D **97**, 053003 (2018); W. H. Chiu, S. C. Leung, T. Liu, K. F. Lyu, and L. T. Wang, J. High Energy Phys. 05 (2018) 081.